Space charge capacitance study of GaP/Si multilayer structures grown by plasma deposition

A.S. Gudovskikh, A Baranov, A Uvarov, D Kudryashov, Jean-Paul Kleider

Space charge capacitance study of GaP/Si multilayer structure grown by plasma deposition

A.S. Gudovskikh[1,2]*, A. I. Baranov[1], A.V. Uvarov[1], D. A. Kudryashov[1], J.-P. Kleider[3,4]

[1]Alferov University, Saint-Petersburg, 194091, Russia

E-mail: gudovskikh@spbau.ru

[2]Saint-Petersburg Electrotechnical University "LETI", 197376, Saint-Petersburg, Russia

[3]Université Paris-Saclay, CentraleSupélec, CNRS, Laboratoire de Génie Electrique et Electronique de Paris, F-91192, Gif-sur-Yvette, France

[4]Sorbonne Université, CNRS, Laboratoire de Génie Electrique et Electronique de Paris, F-75252, Paris, France

Keywords: admittance spectroscopy, DLTS, C-V profiling, band offset, gallium phosphide, silicon

Abstract

Microcrystalline GaP/Si multilayer structures grown on GaP substrates using combination of PE-ALD for GaP and PECVD for Si layers deposition are studied by three main space charge capacitance techniques: *C-V* profiling, admittance spectroscopy (AS) and deep level transient spectroscopy (DLTS), which have been used on Schottky barriers formed on the GaP/Si multilayer structures. *C-V* profiling qualitatively demonstrates an electron accumulation in the Si/GaP wells. However, quantitative determination of the concentration and spatial position of its maximum is limited by the strong frequency dependence of the capacitance caused by electron capture/emission processes in/from the Si/GaP wells. These processes lead to signatures in AS and DLTS with activation energies equal to 0.39±0.05 eV and 0.28±0.05 eV, respectively, that are linked to the energy barrier at the GaP/Si interface. It is shown that the value obtained by AS (0.39±0.05 eV) is related to the response from Si/GaP wells located in the

quasi-neutral region of the Schottky barrier, and it corresponds to the conduction band offset at the GaP/Si interface, while DLTS rather probes wells located in the space charge region closer to the Schottky interface where the internal electric field yields to a lowering of the effective barrier in the Si/GaP wells. Two additional signatures were detected by DLTS, which are identified as defect levels in GaP. The first one is associated to the Si_{Ga}+V_P complex, while the second was already detected in single microcrystalline GaP layers grown by PE-ALD.

1. Introduction

Gallium phosphide (GaP) has the lowest lattice mismatch to Si (0.4%) among III-V binary compounds, which makes it the most attractive nucleation material for the fabrication of a wide variety of different devices based on integration of III-V and Si [1, 2]. For devices where the electrical contact between GaP and Si is involved (optical IC and multijunction solar cells) the properties of the GaP/Si interface are the important issue. Despite the high interest in the integration of III-V and Si and significant amount of reports devoted to the growth of GaP on Si by metal-organic chemical vapor epitaxy (MOVPE), molecular beam epitaxy (MBE) and atomic layer deposition (ALD) there is still a lack of information on GaP/Si interface properties. Indeed, the values of band discontinuity that can be found in the literature are widely scattered. According to several theoretical studies the valence band offset (ΔE_V) was predicted to be in the range of 0.45–0.55 eV [3-5]. Significantly larger values (ΔE_V = 0.8–1.05 eV) with relatively low conduction band offset (ΔE_C =0.09–0.35 eV) were measured by photoemission spectroscopy [6,7] and internal photoemission [8]. On the contrary, lower values (ΔE_V = 0.22-0.3 eV) were measured by X-ray photoelectron spectroscopy and cross-sectional Kelvin probe force microscopy [9]. However, there is almost no report on the study of GaP/Si interface properties by space charge capacitance techniques, that are among the most powerful techniques for interface characterization. The space charge region probing through the interface is required for successful application of the main capacitance techniques. However, commonly used n-GaP/p-Si

heterojunctions are not suitable for such measurements because the space charge region is located in Si far from the interface. Moreover, in case of growth at high temperature (above 700 °C, used for MOVPE) interdiffusion occurs. Phosphorous, which has a higher diffusion coefficient than gallium, diffuses into Si and forms a donor rich region near the interface leading to a buried p/n Si homojunction in p-type Si.

Here the properties of GaP/Si superlattice structures fabricated at low temperature (below 400 °C) are studied using a top Schottky diode. The GaP/Si interfaces are located in the space charge region of the Schottky diode, which makes it possible to investigate them by a variety of space charge capacitance techniques, namely *C-V* profiling, admittance spectroscopy (AS) and deep level transient spectroscopy (DLTS) [10-12]. Moreover, the GaP/Si superlattice structure is of special interest for optoelectronic devices due to the lattice match between GaP and Si and the possibility to control the effective band gap. In Ref. [13] such superlattices were predicted to have a direct gap. Recently, the GaP/Si superlattice structure was proposed as a top cell for tandem multijunction solar cells based on Si [14]. However, it is hard to combine the growth of Si and III-V compounds in a single process from a technological point of view. The strong difference in the growth conditions make the GaP/Si superlattices quite difficult to realize using conventional epitaxial techniques like MOVPE or MBE, explaining why to our knowledge successful GaP/Si superlattice fabrication was not reported so far.

Recently, the growth of microcrystalline GaP/Si multilayer structures was realized using plasma deposition by combining the conventional plasma-enhanced chemical vapour deposition (PECVD) of Si and a plasma-enhanced time modulated process leading to pseudo atomic layer deposition (pseudo PE-ALD) of GaP [15]. The latter was realized with additional hydrogen plasma treatment to etch the remaining excess phosphorous from the chamber walls [16]. This hydrogen plasma treatment led to the formation of voids [15] and the amorphization of GaP [14]. A new hydrogen plasma free PE-ALD process was successfully developed, which allowed us to reach an epitaxial growth of GaP on Si substrates with a smooth surface [17]. Combination of

this PE-ALD process of GaP and PECVD of Si allowed us to avoid the previously observed problems of voids formation and amorphization during the growth of the GaP/Si multilayer structure.

2. Experimental details

The GaP/Si multilayer structures were grown on n-type GaP (100) substrates doped by sulfur ($5\times10^{17}cm^{-3}$). The substrate was treated in HCl:H_2O solution to remove the oxide layer before the deposition. The GaP layers were grown using plasma enhanced atomic layer deposition (PE-ALD) with Ar plasma activation, which provides an epitaxial 2D growth of at least first 20 nm on Si. The main process conditions are given in table 1. For more details refer to [17]. Si was grown using conventional PECVD mode with high hydrogen dilution of SiH_4 (2%), which also provides epitaxial growth on GaP substrates [14]. The whole process was realized at 390°C in the same PECVD Oxford Plasma Lab System 100 chamber with capacitive coupled RF (13.56 MHz) plasma. The GaP/Si multilayer structures consist of 7 Si wells of 2.5 nm thickness separated by GaP barriers of 4.5 nm. Bottom ohmic contact was formed using indium annealed at 350 °C. Finally, Schottky barriers were fabricated by vacuum evaporation of gold on the top of the GaP/Si multilayer structures through a mask with circular holes with a diameter of 0.5 mm. Schematic view of the structure is presented in Figure 1.

Table 1. The main deposition conditions for growth of GaP and Si layers

Parameter	GaP			Si
Growth mode	PE-ALD			PECVD
Deposition duration	50 cycles			22 s
Thickness, nm	4.5			2.5
Step	Phosphorous	Ar plasma	Gallium	-
RF power, W	200	200	-	100
Pressure, mTorr	350	350	350	1900
Gas composition	PH_3/H_2	Ar	5%TMG/H_2	SiH_4/H_2

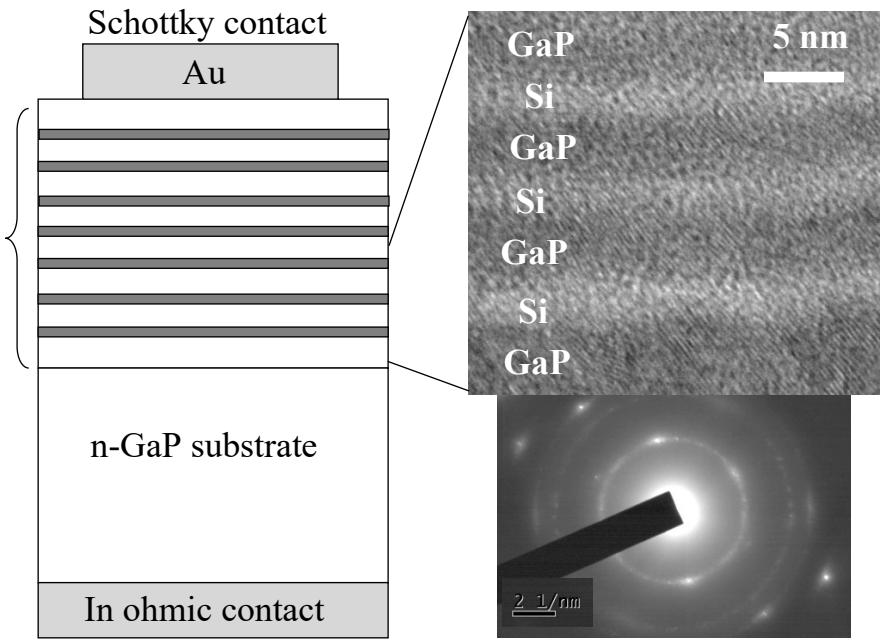

Figure 1. Schematic presentation of the studied structure, TEM image and SAED pattern of the GaP/Si stack.

Transmission electron microscopy (TEM) of the fabricated GaP/Si multilayer structures clearly demonstrates the sequence of the separated layers of GaP and Si (insert of Figure 1) with a sharp contrast. The GaP/Si interfaces are not degraded. The stack of GaP/Si layers has homogeneous microcrystalline structure according to selective area electron diffraction (SAED) (insert of Figure 1). The problem of GaP amorphization during the growth of GaP/Si multilayer structures, which was observed previously [14] for pseudo-PE-ALD of GaP with H_2 plasma treatment, was not detected by TEM for this structure. Significant improvement of the structural properties was achieved using a true PE-ALD process with Ar plasma activation.

C-V and AS measurements were performed using a precision E4980A Keysight LCR-meter in the frequency range from 20 Hz to 2 MHz. An automated setup based on a Boonton-7200B capacitance bridge was used for measurements by the classical DLTS method at 1 MHz. We used two cryostats to allow for measurements in a very broad temperature range; a Janis CCS-400H/204 helium cryostat and a Janis VPF-100 liquid nitrogen cryostat were used to set and control the temperature from 40 to 80 K and from 80 to 340 K, respectively.

3. Results and discussion

Admittance spectroscopy is the simultaneous measurement of capacitance, C, and conductance, G, as a function of frequency, f, and temperature, T, and the results are usually displayed in the form of C-f-T and G/ω-f-T curves, ω being the angular frequency, $\omega = f/2\pi$. Figures 2 and 3 show the results obtained in the temperature ranges of 40-80 K and 80-340 K, respectively. For the low temperature range a step of the capacitance down to extremely low values is observed in C-f-T curves when the frequency increases (Figure 2). This capacitance step is accompanied by a peak of G/ω, both shifting to higher frequency when temperature the increases. Obviously, this behavior is caused by the freeze-out of free carriers in GaP substrate because the dopant is not fully ionized at such temperatures. The activation energy, E_a = 0.07±0.03 eV extracted from the Arrhenius plot of peak frequency of G/ω presented in Figure 4, corresponds well to the ionization energy of S_P (sulfur in phosphorous position) donor level of 0.1 eV reported in [18]. Charge carrier transport deactivation at low temperature (or high frequency) make unreasonable any capacitance measurements in this temperature range.

The admittance spectra measured in the 80-340 K temperature range also exhibit a step in the capacitance accompanied by peak of G/ω (Figure 3). The activation energy calculated from the Arrhenius plot using dC/df or G/ω peak positions is equal to 0.39±0.05 eV (Figure 4). The behavior of the admittance spectra is not changed when a reverse bias is applied to the Schottky diode: the capacitance step positions as well as the activation energy remain the same (within measurement incertitude) up to a reverse bias of 0.8 V. The determination of the activation energy for reverse biases larger than 0.8 V becomes impossible due to the appearance of a large conductance contribution that masks the peak in G/ω and makes the capacitance measurement unreliable. The fact that there is no dependence of activation energy on applied voltage for the observed feature in the C-f-T and G-f-T curves means that it is rather related to the response from

a single energetic level located at 0.39±0.05 eV below E_c in the GaP/Si superlattice or due to the activation of transport over the potential barrier from the wells.

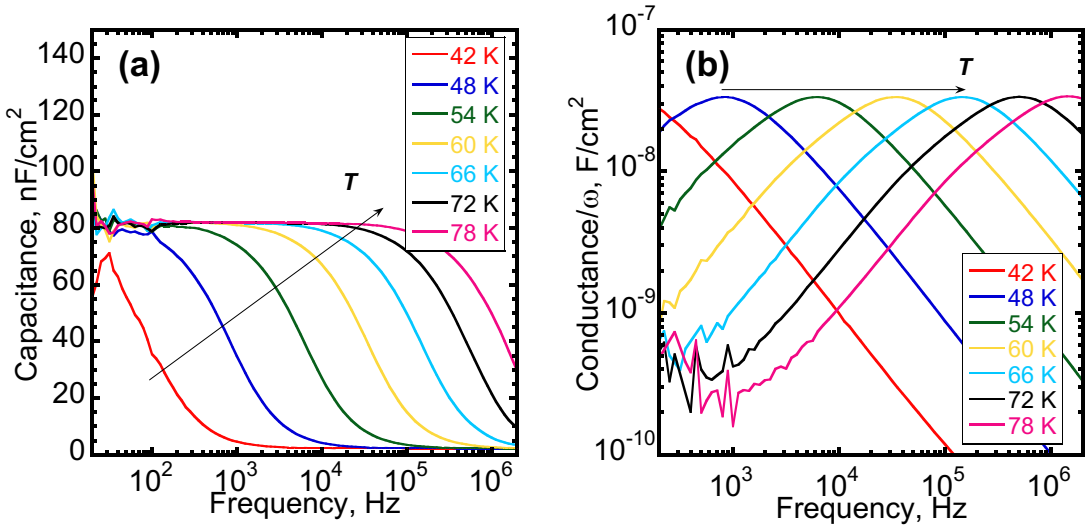

Figure 2. *C-f-T* (a) and *G/ω-f-T* (b) curves measured at zero applied voltage in the 40-80 K temperature range.

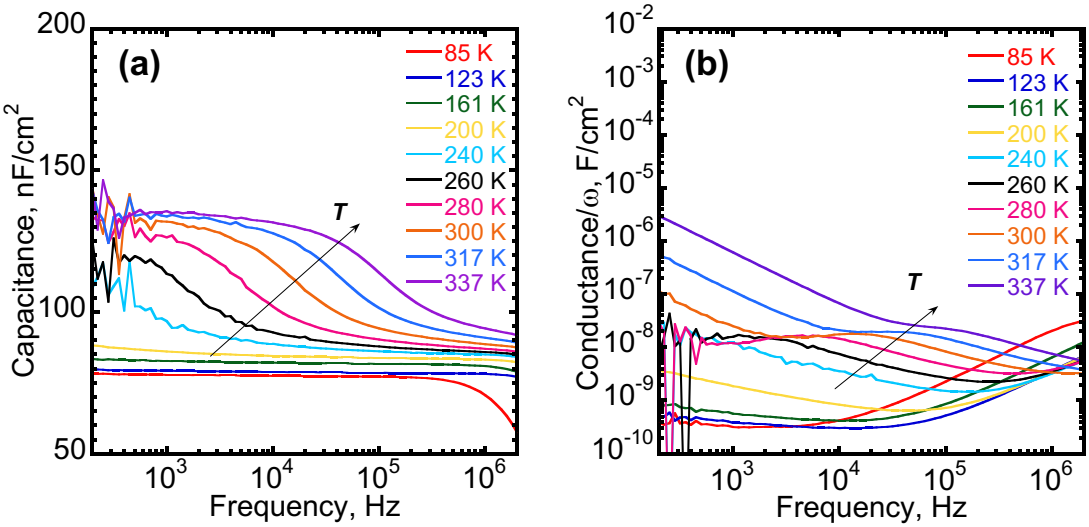

Figure 3. *C-f-T* (a) and *G-f-T* (b) curves measured at zero applied voltage in the 80-340 K temperature range.

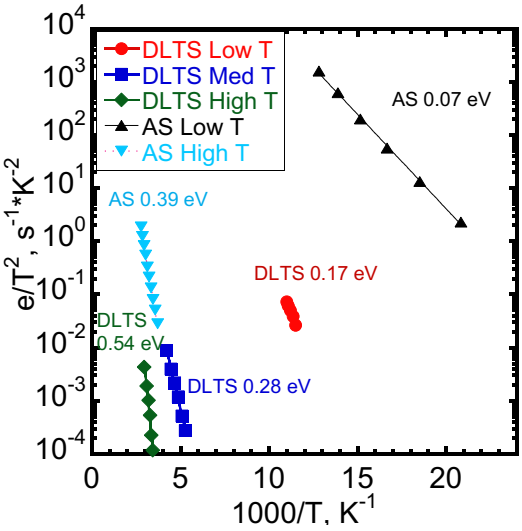

Figure 4. Arrhenius plots of the signatures detected in AS and DLTS. The corresponding activation energies are indicated.

The DLTS measurements were performed at zero bias voltage and with a 50 ms forward bias filling pulse at +2 V. According to the low capacitance value (Figure 3a), at zero voltage the space charge region width is about 50 nm (estimated assuming a permittivity value of 11.1), and, therefore, it is located in the GaP/Si multilayer structure. The positive bias pulse (+2 V) pushes the Schottky diode to flatband conditions and injects electron in the space charge region, which provides the filling of defect states and of the Si wells in the GaP/Si structure within this distance. Such conditions allow one to get a response from the GaP/Si multilayer heterostructure without any contribution from the GaP substrate. The measured DLTS spectra presented in Figure 5 have three series of peaks, which Arrhenius plots have also been included in Figure 4.

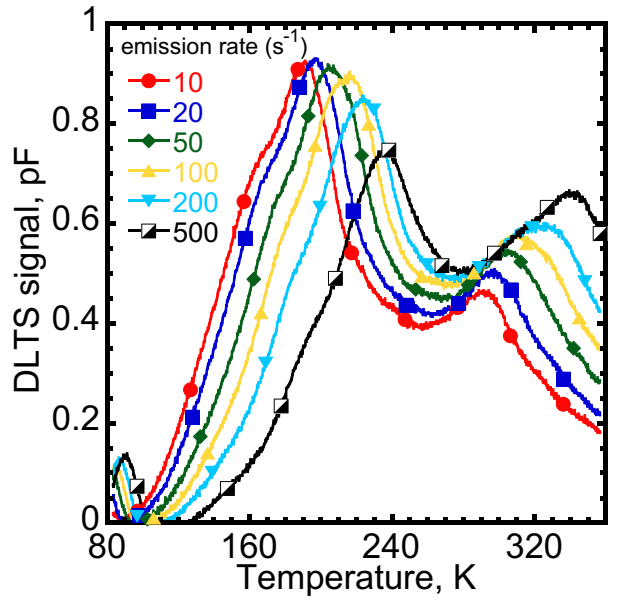

Figure 5. DLTS spectra measured at zero applied voltage in the 80-340 K temperature range for different emission rates, which values are indicated in the graph (in s^{-1}).

The first response observed in the temperature range of 80–100 K with an activation energy of 0.17±0.05 eV (Figure 4) corresponds to a defect level at E_C – 0.17±0.05 eV with a capture cross section of (5–10)×10^{-14} cm^2 and a concentration of (1–3)×10^{15} cm^{-3} (calculated assuming an effective density of states in the conduction band of 1.8×10^{19} cm^{-3}). This level is associated with the incorporation of silicon into GaP leading to the formation of Si_{Ga} + V_P complexes [19]. This type of defect appears under non-equilibrium growth conditions when a large number of gallium and phosphorus vacancies are formed and Si occupies the gallium vacancies. It is a frequently observed defect in GaP layers doped by silicon [20-22]. Silicon doping is expected here in the GaP layers because of Si residuals that can be incorporated during the GaP/Si structure growth.

The second series of peaks is detected in the temperature range of 160–280 K, and it has an activation energy of 0.28±0.05 eV. According to the Arrhenius plots of Figure 4 these DLTS data points are in line with the ones originated with the high temperature signature observed in AS. The slightly lower activation energy compared to 0.39±0.05 eV value extracted from AS will be commented later in this paper.

The third series of peaks obtained at temperatures above 300 K has an activation energy of 0.54±0.05 eV, and it is attributed to the response of a defect in GaP at E_C–0.54±0.05 eV with a capture cross section of $\sigma=(1–4)\times10^{-15}$cm^2 and a concentration of $N_T=(1–10)\times10^{15}$ cm^{-3}. Indeed, a similar defect level was already detected in single microcrystalline GaP layers grown by PE-ALD [23].

Finally, the capacitance versus voltage (*C-V*) measurements were performed. The measurements were carried out at 300 K in the voltage and frequency range from 0 to –4 V and from 50 kHz to 1 MHz, respectively. The obtained *C-V* curves for different frequencies presented in Figure 6 have similar nonlinear behavior with significant difference in absolute values as could be assumed from the *C-f-T* curves (Figure 3a). The concentration profiles, which are presented in Figure 7, were calculated from the measured *C-V* curves according to the procedure described in [10]. The apparent charge carrier concentration profiles for all the frequencies exhibit a well pronounced peak corresponding to electron accumulation in the Si quantum wells. However, the apparent peak electron concentration decreases and its position is shifted towards the surface with decreasing measurement frequency due to the strong frequency dependence of the capacitance at 300 K. Indeed, the measurements at 1 MHz are performed below the capacitance step, while the capacitance drastically increases with decreasing frequency (Figure 3a). Unfortunately, *C-V* measurements at frequencies lower than 50 kHz were not reliable due to the strong contribution of the parasitic conductance, which increases with reverse bias. Thus, the true electron concentration in Si wells and its position cannot be determined accurately by *C-V* profiling.

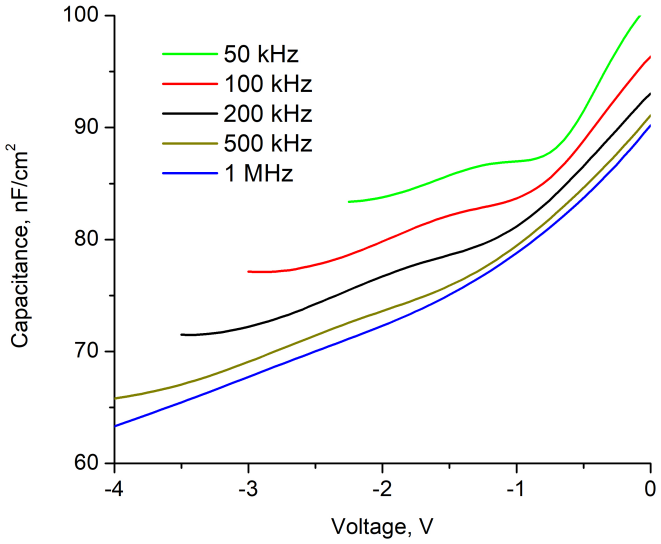

Figure 6. *C-V* curves measured at 300 K for different frequencies.

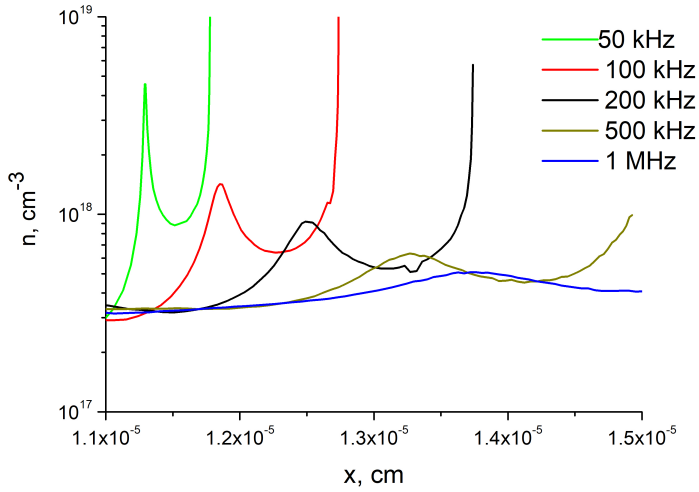

Figure 7. Apparent charge carrier concentration from *C-V* measurements performed at different frequencies at 300 K.

To get insight into the origin of the observed capacitance behavior computer simulations of the *C-V* and admittance spectra were performed using AFORS-HET 2.5 software [24]. First the ideal GaP/Si superlattice structure containing 7 Si quantum wells separated by GaP barrier layers with high electron mobility of 110 $cm^2V^{-1}s^{-1}$ was simulated. An example of the calculated band diagram for the GaP/Si superlattice within the Schottky barrier region is presented in Figure 8. Despite the fact that GaP was not intentionally doped a high Si concentration is expected in GaP due to residual Si remaining in the chamber after deposition of the Si wells. According to our

previous study of Si incorporation and donor doping level performed by electrochemical *C-V* for undoped GaP layers obtained by PE-ALD the concentration of Si could be estimated in the range of 10^{17}- 2×10^{18} cm^{-3}.

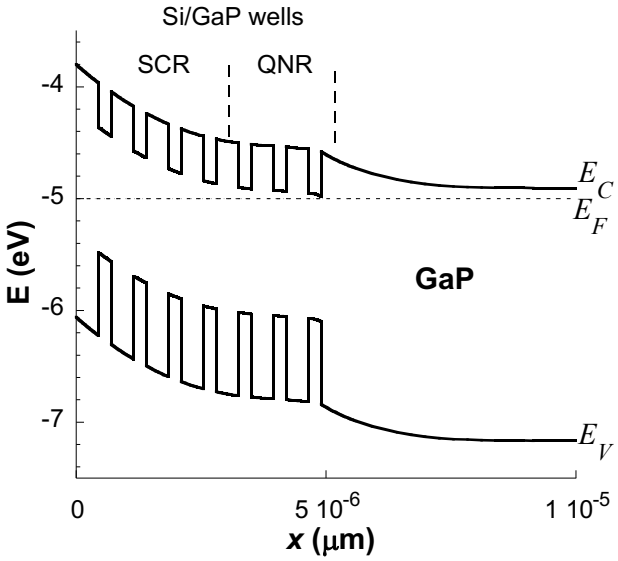

Figure 8. Calculated band diagram of the GaP/Si superlattice within the Schottky barrier region for ΔE_C=0.4 eV and donor doping concentration of GaP barrier layers equal to 10^{18} cm^{-3}. Space charge region (SCR) and quasi-neutral region (QNR) Si/GaP wells are indicated.

The values of the conduction band offset (ΔE_C) and donor doping concentration of GaP layers (N_d) were varied in the simulations. The real electron concentration profiles extracted from the band diagram and the apparent charge carrier concentration profiles calculated from the simulated *C-V* curves using the same procedure as for the experimental data (as described in [10]) for different values of ΔE_C and N_d are presented in Figure 9. An electron accumulation, which occurs in Si wells, can be clearly detected by the *C-V* profiling technique. The concentration of charge carriers in Si wells obviously increases when increasing ΔE_C (Figure 9a). This opens a way for the determination of this band offset by comparing the calculated apparent concentration with the measured one. However, the electron concentration in Si wells strongly depends on the doping level in the GaP barrier layers (Figure 9b), which is not exactly known.

This makes it difficult to determine very accurately ΔE_C from the experimental *C-V* profiling measurements. Moreover, the experimental apparent electron concentration profiles depend on the measured frequency (Figure 7), while for the simulated ideal GaP/Si superlattice structure they are frequency independent in the range of 100-10^6 Hz.

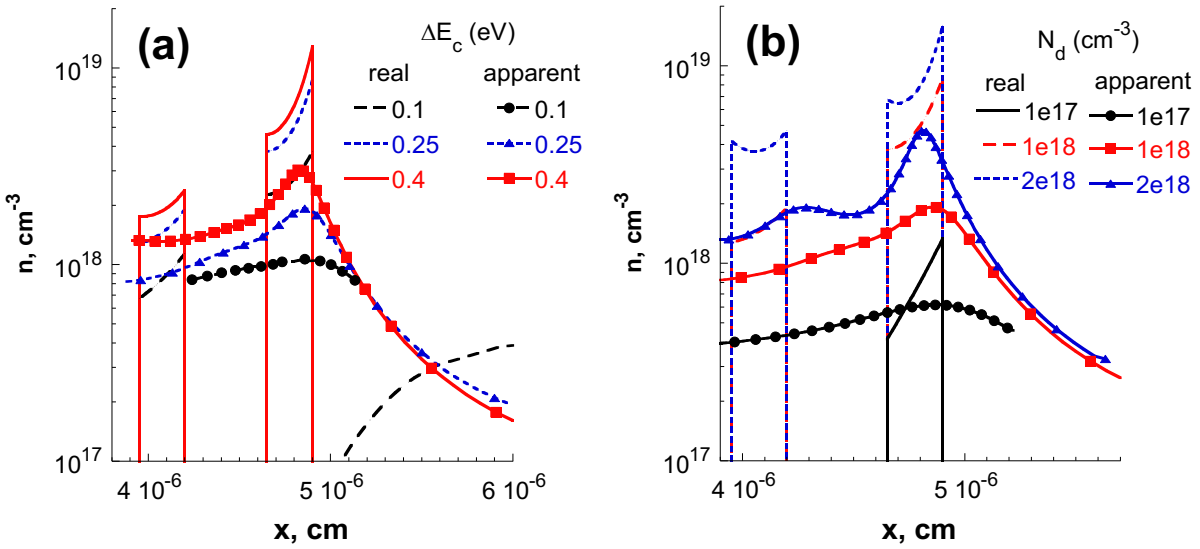

Figure 9. Real and apparent electron concentration profiles calculated from the simulated *C-V* curves with $N_d = 10^{18}$ cm^{-3} for different values of ΔE_C (a) and for $\Delta E_C = 0.25$ eV for various values of N_d (b) with an electron mobility in the GaP barrier layers equal to 110 cm^{2}V^{-1}s^{-1}.

The main difference between the calculated ideal GaP/Si structure and the fabricated one is that experimental GaP layers are microcrystalline instead of monocrystalline. Thus, the mobility of our GaP layers are expected to be significantly lower than that of monocrystalline GaP. This is why a second series of simulations were performed with a low electron mobility of 1 cm^{2}V^{-1}s^{-1} in the GaP barrier layers of the GaP/Si superlattice structure, which band diagram is shown in Figure 8 (ΔE_C =0.4 eV and N_d =10^{18} cm^{-3}). The calculated admittance spectra for this structure are presented in Figure 10. The spectra exhibit a step in the capacitance accompanied by a peak of the G/ω with an activation energy of 0.4 eV, in good agreement with the experimentally deduced value (Figure 3).

For the same GaP/Si structure with low GaP mobility the profiles of apparent charge carrier concentration were calculated using the simulated *C-V* curves for two frequencies (1 kHz and 1 MHz) (Figure 11). At low frequency (1 kHz) the calculated profile corresponds well to the real concentration distribution. However, at higher frequency (1 MHz) the calculated electron concentration in Si wells is much lower and significantly shifted from the surface toward the bulk. The observed frequency dependence of the calculated *C-V* profiles is in good qualitative agreement with the experimental data (Figure 7).

The behavior of the simulated capacitance spectra is related to the activation of the transport through the GaP/Si multi well quasi neutral region (Figure 8). When the temperature is too low or the frequency is too high the total capacitance is equal to two capacitances in series: the space charge capacitance (C_{SCR}) and the capacitance formed by Si/GaP wells in the quasi-neutral region (C_{QNR}) (Figure 10). For higher temperature or lower frequency, which enable electron emission over the GaP barrier the transport through the GaP/Si quasi neutral region is activated. The total capacitance is the equal to the space charge capacitance in this case (Figure 10). The step in the capacitance occurs at the transition frequency, which increases with temperature. In case of high mobility of GaP barrier layers, this capacitance step is shifted to much higher frequency and is not visible in the experimental frequency range.

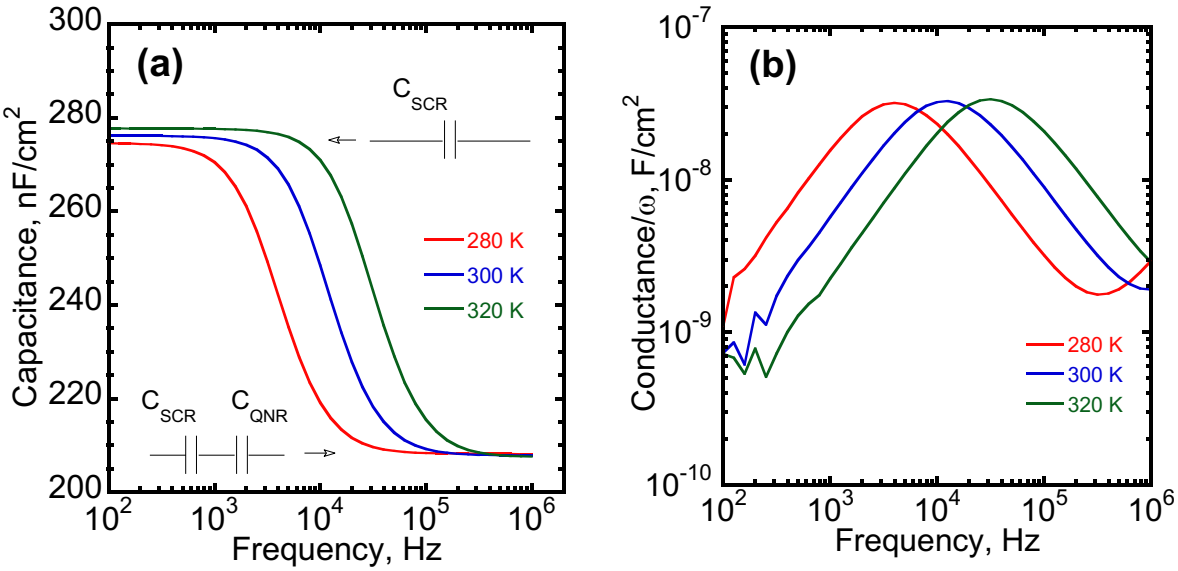

Figure 10. Calculated *C-f-T* (a) and *G/ω-f-T* (b) curves for a GaP/Si superlattice structure with ΔE_C =0.4 eV, donor doping concentration and electron mobility of GaP barrier layers equal to 10^{18} cm^{-3} and 1 $cm^2V^{-1}s^{-1}$, respectively.

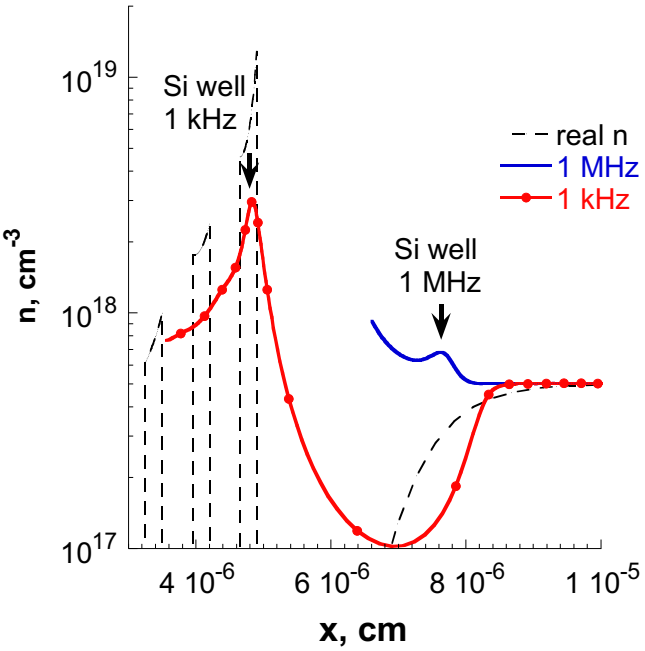

Figure 11. Real and apparent electron concentration profiles calculated from the simulated *C-V* curves for two frequencies (1 kHz and 1 MHz) for the GaP/Si superlattice structure with ΔE_C =0.4 eV, donor doping concentration and electron mobility of GaP barrier layers equal to 10^{18} cm^{-3} and 1 $cm^2V^{-1}s^{-1}$, respectively.

The height of the potential barrier, which should be overcome by electrons in the GaP/Si multi well structure, corresponds to the conduction band offset at the GaP/Si interface (Figure 8). Therefore, the activation energy of the admittance spectra is related to ΔE_C, that was confirmed by the set of simulations where ΔE_C was varied in the range of 0.1-0.4 eV. Thus, admittance spectroscopy provides a way for direct experimental determination of ΔE_C.

The activation energy obtained by DLTS for the same response (0.28±0.05 eV) is about 0.1 eV lower compared to that from admittance spectroscopy. Similarly lower activation energy determined by DLTS compared to that from admittance spectroscopy was reported in Ref [25] for quantum dots levels. One of the possible reasons for the slightly lower activation energy

deduced by DLTS could be related to a lower effective potential barrier due to the electric field in the space charge region. Indeed, the response from DLTS measurements is related to electron emission from Si/GaP wells located in the space charge region, in contrast to admittance spectroscopy where emission occurs from the quasi neutral region. During the forward bias filling pulse of DLTS, the wells in the space charge region are filled with electrons (Figure 12a). When the bias is returned to zero electrons are emitted from the filled Si wells and the capacitance relaxation is measured (Figure 12b). For the wells located in the electric field the potential barrier turns out to be lower (inset of Figure 12b). According to simulations for ΔE_C =0.4 eV the decrease of the potential barrier is of 0.08 eV, in good agreement with the experimentally observed difference in activation energies between AS and DLTS.

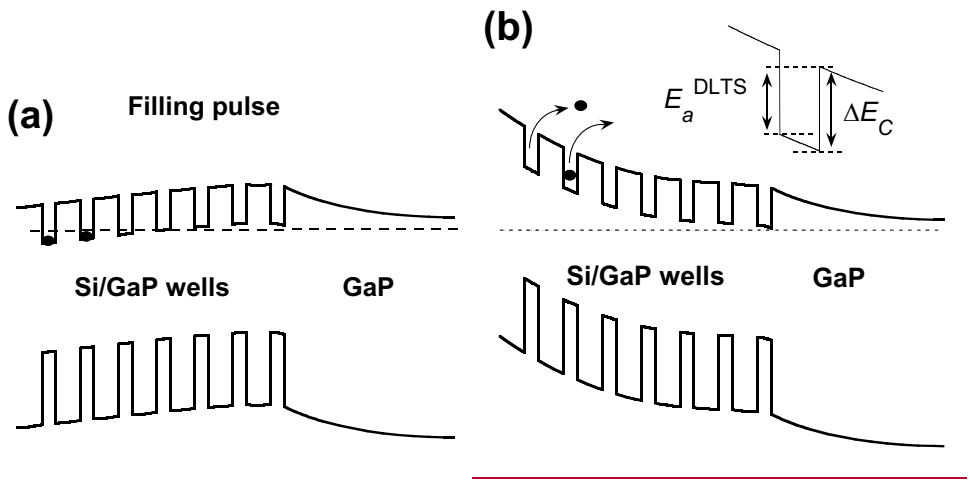

Figure 12. Schematic representation of the band diagram for filling pulse (a) and capacitance relaxation (b) during DLTS measurements. Zoom of the Si/GaP well located in the space charge region.

Thus, the value of the activation energy deduced by admittance spectroscopy is more reliable for ΔE_C determination. Note also that the experimentally obtained value in this work of 0.39±0.05 eV is in good agreement with photoemission measurements of ΔE_V =0.8 eV performed by *P. Perfetti* [6] and corresponds well to our previous transport study of GaP/Si interfaces, which

confirms that the valence band offset at the GaP/Si heterojunction is significantly larger than the conduction band offset [26].

5. Conclusion

A way to determine the band discontinuity for microcrystalline heterojunctions by application of space charge capacitance techniques to a multilayer structure was demonstrated. The conduction band offset at the GaP/Si interface was determined for a microcrystalline GaP/Si multilayer structure using *C-V* profiling, AS and DLTS measurements. An electron accumulation in the Si/GaP wells of the multilayer structure was demonstrated by *C-V* profiling. The electron capture/emission process in Si/GaP wells located in the quasi-neutral region was directly detected by admittance spectroscopy. The activation energy of this process corresponds to conduction band offset at the GaP/Si interface, ΔE_C = 0.39±0.05 eV. Additionally, the capture/emission process from the Si/GaP wells located in the space charge region was detected by DLTS. The lower values of the activation energy (0.28±0.05 eV) determined in this case is associated to the barrier lowering due to internal electric field in the space charge.

Acknowledgements

This work was supported by the Russian Scientific Foundation under Grant № 17-19-01482.

References

[1] *III-V Compound Semiconductors: Integration with Silicon-Based Microelectronics* 2016 (Eds: T. Li, M. Mastro, A. Dadgar), CRC Press.

[2] Feifel M, Ohlmann J, Benick J, Rachow T, Janz S, Hermle M, Dimroth F, Belz J, Beyer A, Volz K, Lackner D, 2017 *IEEE J. Photovoltaics* **7** 502

[3] Lazzouni M E, Peressi M, Baldereschi A 1995 *Appl. Phys. Lett.* **68** 75

[4] Jingguang C, Kaiming Z, Xide X 1994 *Phys. Rev. B* **50**,18167

[5] Romanyuk O, Hannappel T, Grosse F 2013 *Phys. Rev. B* **88** 115312

[6] Perfetti P, Patella F, Sette F, Quaresima C, Capasso C, Savoia A, Margaritondo G 1984 *Phys. Rev. B* **30**, 4533 (https://doi.org/10.1103/PhysRevB.30.4533)

[7] Katnani A D, Margaritondo G 1983 *Phys. Rev. B* **28** 1944 (https://doi.org/10.1103/PhysRevB.28.1944)

[8] Sakata I, Kawanami H 2008 *Appl. Phys. Express* **1** 091201

[9] Saive R, Emmer H, Chen C T, Zhang C, Honsberg C, Atwater H 2018 *IEEE 7th World Conference on Photovoltaic Energy Conversion (WCPEC)*, pp. 2064-2069, (doi: 10.1109/PVSC.2018.8547704)

[10] Forrest S R 1987 Measurements of energy band offsets using capacitance and current measurement techniques *Heterojunction Band Discontinuities* ed F Capasso and G Margaritondo (Amsterdam:North-Holland) pp 311–375

[11] Lang D V 1987 Measurement of band offsets by space charge spectroscopy *Heterojunction Band Discontinuities* ed F Capasso and G Margaritondo (Amsterdam:North-Holland) pp 377-395,

[12] Singh D V,Rim R, Mitchell TO, Hoyt J L, Gibbons J F 1999 *J.Appl.Phys.* **85** 985

[13] Lin-Chung P J 1991 *MRS Proceedings* **220** 589

[14] Gudovskikh A S, Uvarov A V, Morozov I A, Baranov A I, Kudryashov D A, Zelentsov K S 2020 *Materials Today: Proceedings*, , 21, pp. 47—52.

[15] Gudovskikh AS, Uvarov A V, Morozov I A, Baranov A I, Kudryashov D A, Zelentsov K S, Bukatin A S, Kotlyar K P 2018 *Journal of Vacuum Science & Technology A: Vacuum Surfaces and Films.*, **36(2)** 02D408,

[16] Gudovskikh A S, Morozov I A, Uvarov A V, Kudryashov D A, Nikitina E V, Bukatin A S, Nevedomskiy V N, Kleider J-P 2018 *Journal of Vacuum Science & Technology A: Vacuum, Surfaces, and Films* **36**, 021302

[17] Uvarov A V, Gudovskikh A S, Nevedomskiy V N, Baranov A I, Kudryashov D A, Morozov I A, Kleider J-P 2020 *J. Phys. D: Appl. Phys.* **53**, 345105

[18] A. A. Kopylov, A. N. Pikhtin, 1978 *Solid State Comm.* **26** ,735-740 (https://doi.org/10.1016/0038-1098(78)90731-7)

[19] Koltsov G, Yurchuk S Yu, 1994 *Phys. Tech. Semicond.* **28** 1661–1667

[20] Kamiński P, Strupiński W, Roszkiewicz K J. 1991 Cryst. Growth **108**, 699

[21] Skazochkin A V, Krutogolov Y K, Kunakin Y I 1995 *Semicond. Sci.Technol.* **10** 634

[22] Baranov A I, Gudovskikh A S, Egorov A Yu, Kudryashov D A, Le Gall S, Kleider J-P 2020 *J. Appl. Phys.* **128**, 023105 (https://doi.org/10.1063/1.5134681)

[23] Baranov A I, Morozov I A, Uvarov A V, Gudovskikh A S 2019 *J. Phys.: Conf. Ser.* **1410** 012116

[24] Varache R, Leendertz C, Gueunier-Farret M E, Haschke J, Muñoz D, Korte L, 2015 *Solar Energy Materials and Solar Cells* **141** 14–23. (doi:10.1016/j.solmat.2015.05.014)

[25] Anand S, Carlsson N, Pistol M E, Samuelson L, Seifert W 1998 *J.Appl.Phys.* **84** 3747

[26] Gudovskikh A S, Zelentsov K S, Baranov A I, Kudryashov D A, Morozov I A, Nikitina E V, Kleider J-P 2016 *Energy Procedia* **102** 56-63 (doi: 10.1016/j.egypro.2016.11.318)